Lithium Superionic Sulfide Cathode for All-Solid Lithium–Sulfur Batteries

Zhan Lin,[†] Zengcai Liu,[‡] Nancy J. Dudney,[†] and Chengdu Liang[‡,*]

[†]Materials Science and Technology Division and [‡]Center for Nanophase Materials Sciences, Oak Ridge National Laboratory, Oak Ridge, Tennessee 37831-6124, United States

ABSTRACT This work presents a facile synthesis approach for core–shell structured Li_2S nanoparticles with Li_2S as the core and Li_3PS_4 as the shell. This material functions as lithium superionic sulfide (LSS) cathode for long-lasting, energy-efficient lithium–sulfur (Li–S) batteries. The LSS has an ionic conductivity of 10^{-7} S cm^{-1} at 25 °C, which is 6 orders of magnitude higher than that of bulk Li_2S ($\sim 10^{-13}$ S cm^{-1}). The high lithium-ion conductivity of LSS imparts an excellent cycling performance to all-solid Li–S batteries, which also promises safe cycling of high-energy batteries with metallic lithium anodes.

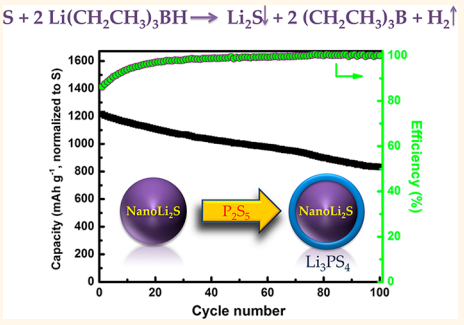

KEYWORDS: batteries · lithium · sulfur · ionic conductivity · cathode

Lithium batteries for use in electrified transportation face two major challenges: (1) limited energy density of the cathode materials based on the intercalation chemistry and (2) safety concerns of high-energy batteries.[1,2] Conventional intercalated cathode materials such as $LiFePO_4$ (170 mAh g^{-1}) and $LiCoO_2$ (136 mAh g^{-1}) have limited energy densities and thus are unable to provide sufficient drive range to electric vehicles on a single charge.[3,4] A promising path for overcoming the challenge of limited energy density of lithium batteries is to move from the traditional intercalation chemistry to innovative conversion chemistry.[5] Lithium–sulfur (Li–S) batteries, based on the following conversion reaction (eq 1)

$$16Li + S_8 \leftrightarrow 8Li_2S \quad (1)$$

can supply a theoretical specific energy of 2500 Wh kg^{-1}, which is 5 times greater than that of lithium-ion (Li-ion) batteries.[6–9]

A typical Li–S battery cell consists of sulfur as the positive electrode and lithium as the negative electrode, with a liquid electrolyte as both the charge transfer medium and the ionic conductor within the sulfur-containing cathode.[10–12] Though much effort has been dedicated to improving the performance of the sulfur cathode,[13–15] the polysulfide shuttle, which results from the dissolution of sulfur species in organic liquid electrolytes, is still a tough challenge in Li–S batteries. The polysulfide shuttle is the migration of the sulfur species from the cathode to the anode, resulting in problems inherent for conventional Li–S batteries, such as the loss of active material, corrosion of lithium anode, and short cycle life of the sulfur-based electrode.[9,16] Moreover, the use of elemental lithium as the anode in Li–S batteries still remains a problem. Serious safety concerns are associated with cycling highly reactive lithium metal in flammable organic electrolytes; lithium dendrites that form in battery cycling penetrate the separator and cause fire hazards.

To promote high performance and alleviate safety concerns of Li–S batteries, this research introduces an all-solid configuration of Li–S batteries with lithium sulfide (Li_2S) as a prelithiated cathode, which avoids the direct use of metallic lithium as the anode. Li_2S has a favorable high theoretical capacity of 1166 mAh g^{-1}, which is far above that of the commonly used $LiFePO_4$ and $LiCoO_2$.[17–19] A solid electrolyte is utilized to deliver enhanced safety by eliminating the highly flammable liquid electrolytes. More importantly, the solid electrolyte eliminates the possibility of the migration of sulfur species and thus promises a long cycle life of Li–S batteries. With the emergence of solid electrolytes with ionic conductivities comparable to that of liquid electrolytes,[20] all-solid Li–S batteries promise to be the next

* Address correspondence to liangcn@ornl.gov.

Received for review January 24, 2013 and accepted February 21, 2013.

Published online February 22, 2013
10.1021/nn400391h

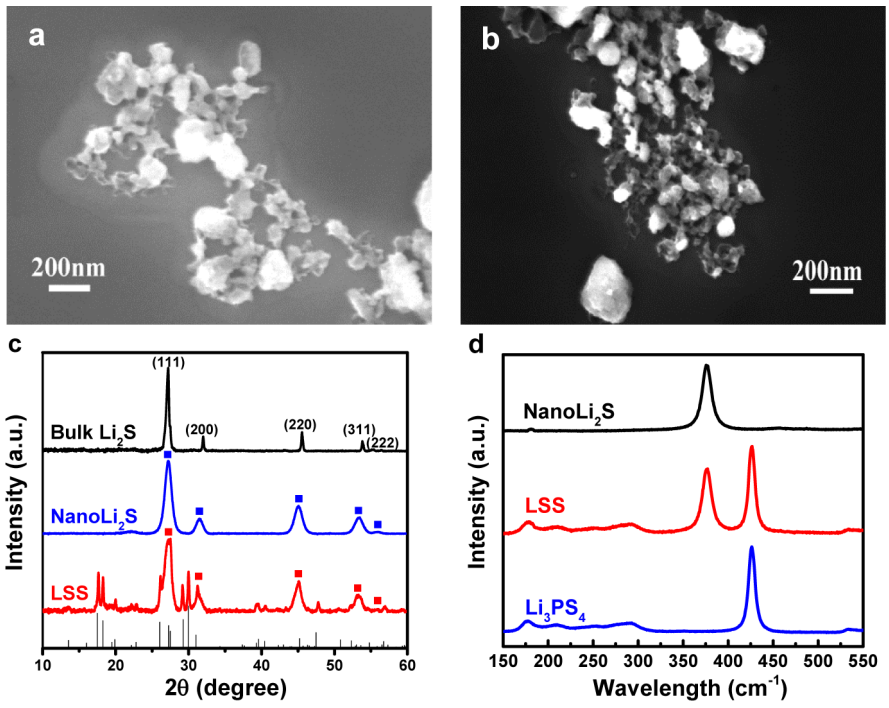

Figure 1. Structural characterization: (a,b) micrographs of the NanoLi$_2$S and LSS, (c) XRD patterns (the symbol ■ identifies the peaks from Li$_2$S), and (d) Raman spectra.

breakthrough for electric energy storage.[21−23] Significant challenges for cycling all-solid Li−S batteries lie in the poor electronic and ionic conductivities of Li_2S. Although the electronic conductivity of the Li_2S cathode can be improved by the addition of carbon to the cathode,[24,25] its ionic conductivity cannot be significantly improved by simply mixing with solid electrolytes. Herein, we present a facile method for synthesizing a sulfide cathode with an enhancement in ionic conductivity by 6 orders of magnitude. This lithium superionic sulfide (LSS) cathode with excellent cyclability was prepared by coating nanostructured lithium sulfide (NanoLi$_2$S) with lithium phosphorus sulfide (Li_3PS_4).

RESULTS AND DISCUSSION

The NanoLi$_2$S was prepared by reacting elemental sulfur (S) with lithium triethylborohydride ($LiEt_3BH$) in tetrahydrofuran (THF) (eq 2):

$$S + 2Li(CH_2CH_3)_3BH \rightarrow Li_2S\downarrow + 2(CH_2CH_3)_3B + H_2\uparrow \quad (2)$$

Aggregates of nanoparticles were precipitated from the THF solution (Figure 1a). The average size of the aggregates is 30−50 nm in diameter, though some large pieces (*e.g.*, ≥200 nm) are also found. The as-synthesized material was identified as a pure phase of Li_2S by X-ray diffraction (XRD): 27.2° (111), 31.6° (200), 45.1° (220), 53.5° (311), and 56.0° (222), respectively (Figure 1c).[26] The XRD of the nanoparticles shows significant peak broadening compared to the bulk Li_2S. The estimated crystallite (or particle) size is 9 nm based on the peak broadening of the XRD pattern. The N_2 adsorption/desorption measurement of the as-synthesized NanoLi$_2$S presents a type IV isotherm with a hysteresis loop that features the mesoporosity of the agglomerates (Supporting Information Figure S1). The Brunauer−Emmett−Teller (BET) surface area is 270 m^2/g, which is consistent with the particle size calculated by XRD.

As expected, the ionic conductivity of the NanoLi$_2$S was enhanced by 2 orders of magnitude compared to that of the bulk Li_2S (Figure 2). The reduced particle size and increased defects of the NanoLi$_2$S account for the boost in ionic conductivity.[27] A surface reaction of NanoLi$_2$S with P_2S_5 in THF confers a superionic conducting coating of lithium phosphorus sulfide (Li_3PS_4)[28,29] on NanoLi$_2$S (eq 3).

$$3Li_2S + P_2S_5 \rightarrow 2Li_3PS_4 \quad (3)$$

The coating further improved the ionic conductivity of NanoLi$_2$S by 4 orders of magnitude, that is, from 10^{-11} to 10^{-7} S cm^{-1} at 25 °C (Figure 2), thus rendering the material a lithium superionic sulfide (LSS).

The morphology of the LSS is similar to that of NanoLi$_2$S, except for a slight increase in particle size due to of the formation of Li_3PS_4 coating on NanoLi$_2$S (Figure 1b). Remarkable peaks are found in the Raman spectra in the wavenumber range of 150 to 550 cm^{-1} (Figure 1d). The strong peak at 375 cm^{-1} appears as evidence of the stretching vibration of the Li−S bond in Li_2S. The predominate peak at 425 cm^{-1} is due to the symmetric stretching of the P−S bond PS_4^{3-}, and weak peaks at 174 and 295 cm^{-1} are from the stretching vibrations of the P−S bond in PS_4^{3-} ions with T_d

symmetry, which confirms the formation of Li_3PS_4 after coating.[30,31] Because of the extreme sensitivity of the β-Li_3PS_4 shell to air and moisture, a publication-quality transmission electron micrograph (TEM) was not attainable. Nevertheless, weak signals of β-Li_3PS_4 were identified in the XRD pattern of the LSS (Figure 1c), while much stronger signals were present on the Raman spectrum of the LSS. Since Raman is sensitive to surface coating and X-ray penetrates through the nanoparticles, the difference in relative signal strengths in Raman and XRD confirms a core−shell structure, in which NanoLi_2S is the core and the air-sensitive β-Li_3PS_4 is the shell.

Excellent cycling performance was demonstrated using the LSS and NanoLi_2S as the cathode materials for Li−S batteries at 60 °C. It should be noted that the temperature of 60 °C was chosen since the ionic conductivity of Li_3PS_4 solid electrolyte is relatively low at room temperature (1×10^{-4} S cm^{-1}). The LSS cathode shows an initial discharge capacity of 848 mAh g^{-1} (based on the lithium sulfide) or 1216 mAh g^{-1} (based on the sulfur content), which accounts for 73% utilization based on the theoretical maximum of 1166 mAh g^{-1} for Li_2S. Though slight capacity fading is observed before 30 cycles, the discharge capacity stabilizes at 594 mAh g^{-1} (unless otherwise noted, the capacities hereafter are normalized to the lithium sulfide; for convenience, the normalized capacities based on the sulfur content are also shown in Figure 3) after 100 cycles, which indicates a capacity retention of 70%. The experimental cell has a high initial Coulombic efficiency of 86% and the Coulombic efficiency of 100% after 30 cycles. Such a high Coulombic efficiency indicates the elimination of the polysulfide shuttle, which has been proven to be the main cause of low Coulombic efficiency in traditional Li−S battery cells when using liquid electrolytes. In comparison, the NanoLi_2S cathode shows an initial discharge capacity of 569 mAh g^{-1} (Figure 3a) and the initial Coulombic efficiency of 88% (Figure 3b). The reversibility gradually increases from the initial 88 to 100% after 30 cycles. After 100 cycles, the capacity is stable at 402 mAh g^{-1}, which indicates a capacity retention of 71%. It should be noted that bulk Li_2S cannot be charged/discharged under the same conditions due to its large particle size and poor ionic conductivity.

While the cyclability of batteries made from LSS is greater than that of batteries made from NanoLi_2S,

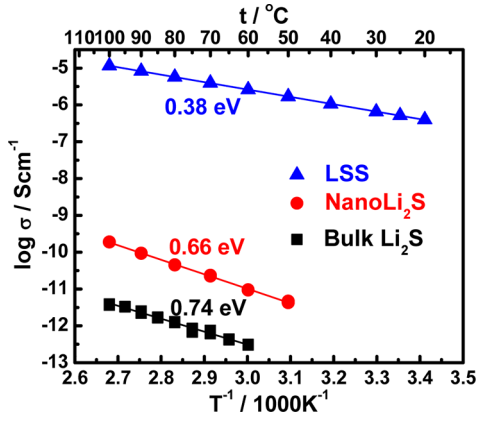

Figure 2. Temperature dependency of ionic conductivities of the bulk Li_2S, NanoLi_2S, and LSS.

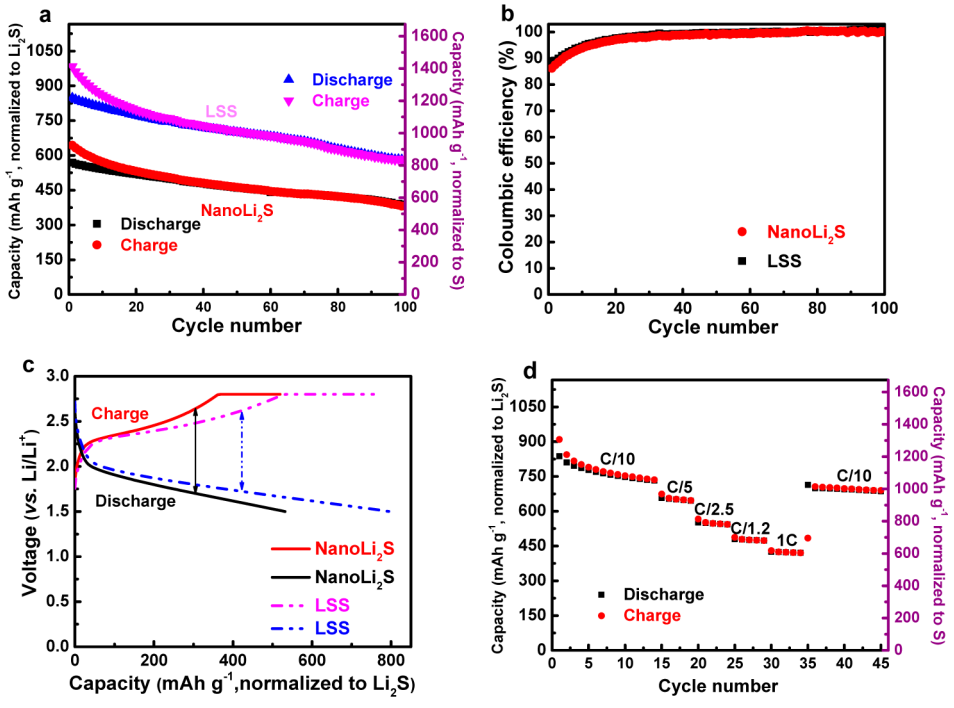

Figure 3. Electrochemical evaluation of NanoLi_2S and LSS as the cathode materials for all-solid Li−S batteries at 60 °C: (a) cycling performance at the rate of C/10. (b) Coulombic efficiency. (c) Representative voltage profiles. (d) Rate performance of the LSS cathode from C/10 to 1C.

which is much greater than that of batteries made from NanoLi$_2$S, following the same trend as the ionic conductivity, it appears that the ionic conductivity of the cathode material is crucial to the cyclability of the batteries. Among these three sulfides, the LSS shows the best cycling performance, which is attributed to its high ionic conductivity and small particle size. The excellent cycling performance of LSS is also due to the preserved electrode integrity under intensive cycling without using liquid electrolytes that causes the migration of sulfur through the polysulfide shuttle (Figure S2). No obvious change in morphology was observed before or after the LSS cathode was cycled at 60 °C for 100 cycles. The voltage profiles of the NanoLi$_2$S and LSS are shown in Figure 3c. Unlike the two-plateau feature in the voltage profile of conventional Li−S batteries with liquid electrolytes, only one plateau was observed in the all-solid Li−S batteries. Large potential hystereses are always observed in all-solid Li−S batteries due to the relatively low ionic conductivity of solid electrolyte as compared to liquid electrolytes and high interfacial resistance at the solid−solid interfaces. It worth noting that the potential hysteresis of the LSS is greatly reduced compared to that of the NanoLi$_2$S, while the energy efficiency of the LSS electrode is enhanced from 65 to 82%. The superior performance of LSS is ascribed to its enhanced ionic conductivity (Figure 2) after the coating of Li_3PS_4 and reduced interfacial resistance at the electrode−electrolyte interface. Excellent rate performance was demonstrated on the full cell with LSS as the cathode (Figure 3d). While the current density increases from C/10 to 1C, the capacity of the LSS decreases slightly. The cell shows a reversible capacity of 435 mAh g^{-1} at 1C after 30 cycles at various rates, and further cycling at a low rate of C/10 brings it back to a reversible capacity of 720 mAh g^{-1}.

CONCLUSION

In summary, a facile synthesis approach of Li_2S nanoparticles was discovered by the reaction of elemental sulfur with lithium triethylborohydride in THF. The reduced particle size improved the ionic conductivity of NanoLi$_2$S by 2 orders of magnitude compared to the bulk Li_2S. The improved ionic conductivity enables NanoLi$_2$S to be cycled in an all-solid battery configuration. Exposure of the surface of NanoLi$_2$S with P_2S_5 results in a core−shell structure of $Li_2S@Li_3PS_4$, which is a superionic conductor, LSS. The high ionic conductivity and reduced particle size of LSS impart an excellent cyclability and rate capability to all-solid Li−S batteries. The ionic conductivity of cathode materials is identified as the key parameter for all-solid Li−S batteries. Although advances have been reported in systems using Li_2S in conventional Li−S batteries with liquid electrolytes, significant challenges still remain such as the migration of sulfur through polysulfide shuttle and the safety concerns of cycling metallic lithium in flammable liquid electrolytes.[17−19] With a paradigm shift from a conventional battery configuration to all-solid batteries, the above challenges with liquid electrolytes are completely eliminated. However, the all-solid batteries face new challenges of low ionic conductivity and high interfacial resistance. This research introduces the approach of solving these problems through innovative nanostructured materials with enhanced ionic conductivity and reduced interfacial resistance.

EXPERIMENTAL SECTION

Sample Preparation. The NanoLi$_2$S was synthesized through a solution-based reaction of elemental sulfur with 1.0 M Li-$(CH_2CH_3)_3BH$ solution in THF. Sulfur was first dissolved and then precipitated out as nanoparticles of NanoLi$_2$S. The collected NanoLi$_2$S was washed, centrifuged, and heat-treated at 140 °C under vacuum for 2 h prior to use. The LSS was prepared by redispersing the NanoLi$_2$S in THF and then stirring with P_2S_5 in a molar ratio of 10:1. β-Li_3PS_4 solid electrolyte was synthesized using a procedure described in our previous publication.[29] Bulk Li_2S was purchased from Sigma-Aldrich and used as received. Solid electrolyte pellets were prepared by pressing 120 mg of β-Li_3PS_4 on top of a lithium-coated Ni foil in a 0.5 in. diameter die set. The Ni foil functions as the current collector of the anode. All pellets were pressed under 300 MPa. The cathode slurry was prepared by mixing 65 wt % active materials (bulk Li_2S, Nano-Li_2S, or LSS) with 25 wt % WVA-1500 carbon (MeadWestvaco Corporation) and 10 wt % PVC binder (Sigma-Aldrich) in THF. The mixtures were stirred for 0.5 h to form a homogeneous slurry. The cathode slurry was coated on the open side of the solid electrolyte pellet. For the measurements of ionic conductivity, pellets of the bulk Li_2S, NanoLi$_2$S, and LSS were prepared by dry-pressing of 120 mg of material in a 0.5 in. (1.27 cm) die set under 300 MPa by using carbon-coated aluminum foil (a sample from Exopack) as the current collector. Due to the extreme sensitivity of Li_2S to the air and moisture, all of the experiments were conducted in an argon-gas-filled glovebox.

Electrochemical Evaluation. The ionic conductivity measurements were conducted in the frequency range of 10 MHz to 1 Hz with the amplitude of 10 mV using a frequency response analyzer (Solartron 1260). Swagelok cells were used to evaluate the cycling performance. Charge and discharge cycles were carried out using a Maccor 4000 series battery tester at a current density of 0.02 mA cm^{-2} (C/10) between the cutoff potentials of 1.5−2.8 V *vs* Li/Li$^+$. At the end of charging cycle, the charge potential was held at a constant voltage of 2.8 V while the current was dropped to 10% of the charging current. The current densities of 0.04 (C/5), 0.075 (C/2.5), 0.15 (C/1.2), and 0.2 (1C) mA cm^{-2} were applied to measure the rate performance of the LSS cathode. The loading of the cathode material was 0.2−0.5 mg cm^{-2}. The calculations of specific charge/discharge capacities were based on the mass of lithium sulfide or sulfur.

Structural Characterization. The morphologies of the cathode before and after cycling were examined using a field emission scanning electron microscope (FE-SEM) (Zeiss Merlin) at 15 kV. The elemental maps of carbon, sulfur, and phosphorus were taken using the energy-dispersive spectroscope of the FE-SEM. X-ray diffraction (XRD) analysis was performed using a PANalytical X'pert PRO 2-circle X-ray diffractometer with a Cu Kα source ($\lambda \approx 1.5418$ Å). Raman spectroscopy was recorded from 600 to

100 cm^{-1} on a Renishaw Confocal MicroRaman spectrometer at room temperature. A green laser with wavelength of 532 nm was used for Raman excitation.

Conflict of Interest: The authors declare no competing financial interest.

Acknowledgment. This research was sponsored by U.S. Department of Energy (DOE)/Energy Efficiency and Renewable Energy (EERE) through Vehicle Technologies Office. The investigation of the ionic conductivity of these new compounds and the preparation of solid electrolytes were supported by the Division of Materials Science and Engineering, Office of Basic Energy Sciences U.S. Department of Energy (DOE). The synthesis and characterization were conducted at the Center for Nanophase Materials Sciences, which is sponsored at Oak Ridge National Laboratory by the Division of Scientific User Facilities, U.S. DOE.

Supporting Information Available: Figure of N_2 adsorption/desorption measurements, SEM images, and elemental maps of the cathode. This material is available free of charge *via* the Internet at http://pubs.acs.org.

REFERENCES AND NOTES

1. Armand, M.; Tarascon, J. M. Building Better Batteries. *Nature* **2008**, *451*, 652–657.
2. Tarascon, J. M.; Armand, M. Issues and Challenges Facing Rechargeable Lithium Batteries. *Nature* **2001**, *414*, 359–367.
3. Goodenough, J. B.; Kim, Y. Challenges for Rechargeable Li Batteries. *Chem. Mater.* **2010**, *22*, 587–603.
4. Ji, L. W.; Lin, Z.; Alcoutlabi, M.; Zhang, X. W. Recent Developments in Nanostructured Anode Materials for Rechargeable Lithium-Ion Batteries. *Energy Environ. Sci.* **2011**, *4*, 2682–2699.
5. Bruce, P. G.; Freunberger, S. A.; Hardwick, L. J.; Tarascon, J. M. Li-O_2 and Li-S Batteries with High Energy Storage. *Nat. Mater.* **2012**, *11*, 19–29.
6. Ji, X. L.; Lee, K. T.; Nazar, L. F. A Highly Ordered Nanostructured Carbon–Sulphur Cathode for Lithium–Sulphur Batteries. *Nat. Mater.* **2009**, *8*, 500–506.
7. Lin, Z.; Liu, Z.; Fu, W.; Dudney, N. J.; Liang, C. Phosphorous Pentasulfide as a Novel Additive for High-Performance Lithium-Sulfur Batteries. *Adv. Funct. Mater.* **2013**, *23*, 1064–1069.
8. Jayaprakash, N.; Shen, J.; Moganty, S. S.; Corona, A.; Archer, L. A. Porous Hollow Carbon@Sulfur Composites for High-Power Lithium–Sulfur Batteries. *Angew. Chem., Int. Ed.* **2011**, *50*, 5904–5908.
9. Liang, C. D.; Dudney, N. J.; Howe, J. Y. Hierarchically Structured Sulfur/Carbon Nanocomposite Material for High-Energy Lithium Battery. *Chem. Mater.* **2009**, *21*, 4724–4730.
10. Guo, J. C.; Xu, Y. H.; Wang, C. S. Sulfur-Impregnated Disordered Carbon Nanotubes Cathode for Lithium–Sulfur Batteries. *Nano Lett.* **2011**, *11*, 4288–4294.
11. Xin, S.; Gu, L.; Zhao, N. H.; Yin, Y. X.; Zhou, L. J.; Guo, Y. G.; Wan, L. J. Smaller Sulfur Molecules Promise Better Lithium–Sulfur Batteries. *J. Am. Chem. Soc.* **2012**, *134*, 18510–18513.
12. Zhang, S. S.; Read, J. A. A New Direction for the Performance Improvement of Rechargeable Lithium/Sulfur Batteries. *J. Power Sources* **2012**, *200*, 77–82.
13. Wang, J.; Chew, S. Y.; Zhao, Z. W.; Ashraf, S.; Wexler, D.; Chen, J.; Ng, S. H.; Chou, S. L.; Liu, H. K. Sulfur–Mesoporous Carbon Composites in Conjunction with a Novel Ionic Liquid Electrolyte for Lithium Rechargeable Batteries. *Carbon* **2008**, *46*, 229–235.
14. Wang, J. L.; Yang, J.; Wan, C. R.; Du, K.; Xie, J. Y.; Xu, N. X. Sulfur Composite Cathode Materials for Rechargeable Lithium Batteries. *Adv. Funct. Mater.* **2003**, *13*, 487–492.
15. Xiao, L. F.; Cao, Y. L.; Xiao, J.; Schwenzer, B.; Engelhard, M. H.; Saraf, L. V.; Nie, Z. M.; Exarhos, G. J.; Liu, J. A Soft Approach To Encapsulate Sulfur: Polyaniline Nanotubes for Lithium–Sulfur Batteries with Long Cycle Life. *Adv. Mater.* **2012**, *24*, 1176–1181.
16. Mikhaylik, Y. V.; Akridge, J. R. Polysulfide Shuttle Study in the Li/S Battery System. *J. Electrochem. Soc.* **2004**, *151*, A1969–A1976.
17. Hassoun, J.; Scrosati, B. A High-Performance Polymer Tin Sulfur Lithium Ion Battery. *Angew. Chem., Int. Ed.* **2010**, *49*, 2371–2374.
18. Yang, Y.; McDowell, M. T.; Jackson, A.; Cha, J. J.; Hong, S. S.; Cui, Y. New Nanostructured Li_2S/Silicon Rechargeable Battery with High Specific Energy. *Nano Lett.* **2010**, *10*, 1486–1491.
19. Cai, K. P.; Song, M. K.; Cairns, E. J.; Zhang, Y. G. Nanostructured Li_2S-C Composites as Cathode Material for High-Energy Lithium/Sulfur Batteries. *Nano Lett.* **2012**, *12*, 6474–6479.
20. Kamaya, N.; Homma, K.; Yamakawa, Y.; Hirayama, M.; Kanno, R.; Yonemura, M.; Kamiyama, T.; Kato, Y.; Hama, S.; Kawamoto, K.; *et al.* A Lithium Superionic Conductor. *Nat. Mater.* **2011**, *10*, 682–686.
21. Kobayashi, T.; Imade, Y.; Shishihara, D.; Homma, K.; Nagao, M.; Watanabe, R.; Yokoi, T.; Yamada, A.; Kanno, R.; Tatsumi, T. All Solid-State Battery with Sulfur Electrode and Thio-LISICON Electrolyte. *J. Power Sources* **2008**, *182*, 621–625.
22. Mizuno, F.; Hama, S.; Hayashi, A.; Tadanaga, K.; Minami, T.; Tatsumisago, M. All Solid-State Lithium Secondary Batteries Using High Lithium Ion Conducting Li_2S-P_2S_5 Glass-Ceramics. *Chem. Lett.* **2002**, 1244–1245.
23. Hassoun, J.; Scrosati, B. Moving to a Solid-State Configuration: A Valid Approach To Making Lithium–Sulfur Batteries Viable for Practical Applications. *Adv. Mater.* **2010**, *22*, 5198–5201.
24. Shim, J.; Striebel, K. A.; Cairns, E. J. The Lithium/Sulfur Rechargeable Cell—Effects of Electrode Composition and Solvent on Cell Performance. *J. Electrochem. Soc.* **2002**, *149*, A1321–A1325.
25. Gao, J.; Lowe, M. A.; Kiya, Y.; Abruna, H. D. Effects of Liquid Electrolytes on the Charge-Discharge Performance of Rechargeable Lithium/Sulfur Batteries: Electrochemical and *In Situ* X-ray Absorption Spectroscopic Studies. *J. Phys. Chem. C* **2011**, *115*, 25132–25137.
26. Nagao, M.; Hayashi, A.; Tatsumisago, M. High-Capacity Li_2S-Nanocarbon Composite Electrode for All-Solid-State Rechargeable Lithium Batteries. *J. Mater. Chem.* **2012**, *22*, 10015–10020.
27. Maier, J. Nanoionics: Ion Transport and Electrochemical Storage in Confined Systems. *Nat. Mater.* **2005**, *4*, 805–815.
28. Hayashi, A.; Hama, S.; Morimoto, H.; Tatsumisago, M.; Minami, T. Preparation of Li_2S-P_2S_5 Amorphous Solid Electrolytes by Mechanical Milling. *J. Am. Ceram. Soc.* **2001**, *84*, 477–479.
29. Liu, Z.; Fu, W.; Payzant, E. A.; Yu, X.; Wu, Z.; Dudney, N. J.; Kiggans, J.; Hong, K.; Rondinone, A. J.; Liang, C. Anomalous High Ionic Conductivity of Nanoporous β-Li_3PS_4. *J. Am. Chem. Soc.* **2013**, *135*, 975–978.
30. Mizuno, F.; Hayashi, A.; Tadanaga, K.; Tatsumisago, M. New, Highly Ion-Conductive Crystals Precipitated from Li_2S-P_2S_5 Glasses. *Adv. Mater.* **2005**, *17*, 918–921.
31. Muller, A.; Mohan, N.; Cristoph, P.; Tossidis, I.; Drager, M. Investigation of Vibrational-Spectra of PS_4^{3-}, CS_3^{2-}, CS_2Se^{2-}, $CSSe_2^{2-}$, CSe_3^{2-}, BCl_2Br and $BClBr_2$. *Spectrochim. Acta, Part A* **1973**, *A29*, 1345–1356.